

Nickel/Lanthanide Single-Molecule Magnets: $\{\text{Ni}_3\text{Ln}\}$ “Stars” with a Ligand Derived from the Metal-Promoted Reduction of Di-2-pyridyl Ketone under Solvothermal Conditions

Constantinos G. Efthymiou,^{†‡} Theocharis C. Stamatatos,[†] Constantina Papatriantafyllopoulou,[†] Anastasios J. Tasiopoulos,[§] Wolfgang Wernsdorfer,[⊥] Spyros P. Perlepes,^{*,‡} and George Christou^{*,†}

[†]Department of Chemistry, University of Florida, Gainesville, Florida 32611-7200, United States,

[‡]Department of Chemistry, University of Patras, 26504 Patras, Greece, [§]Department of Chemistry, University of Cyprus, Nicosia 1678, Cyprus, and [⊥]Institut Louis Néel, CNRS, and Université J. Fourier, BP 166, 38042 Grenoble Cedex 9, France

Received July 27, 2010

Unusual $\{\text{Ni}^{\text{II}}_3\text{Ln}^{\text{III}}(\mu\text{-OR})_6\}^{3+}$ complexes with a “star” topology have been prepared with ligands derived from the metal-promoted reduction of di-2-pyridyl ketone under solvothermal conditions; the Dy^{III} member shows weak single-molecule-magnet behavior.

Most single-molecule magnets (SMMs) are 3d metal clusters, with the majority of them being Mn clusters containing at least some Mn^{III} centers.¹ Several groups, including our own, have recently been exploring mixed 3d/4f metal complexes, and particularly Mn/Ln ones (Ln = lanthanide), as attractive routes to new SMMs.² The strategy is obviously to take advantage of the Ln^{III} ion’s significant spin and/or its large anisotropy to generate SMMs with properties distinctly different from those of the homometallic ones. Indeed, there are now several Mn/Ln SMMs,³ but also SMMs resulting from the combination of other 3d metal and Ln ions.⁴ We are targeting new synthetic routes that might yield low-nuclearity 3d metal/Ln^{III} complexes that are more amenable to an

Chart 1. Organic Groups Discussed in the Text



in-depth analysis of the nature and strength of their exchange interactions.⁵

The mono/dianions of the (py)₂C(OR)(OH) hemiketal and *gem*-diol forms of di-2-pyridyl ketone, (py)₂CO (Chart 1; R = H, Me, Et), are excellent sources of 3d homometallic clusters.⁶ We have recently extended their use to mixed 3d/4f metal chemistry by reporting Ni₂Ln complexes.⁷ The vast majority of 3d/4f metal clusters in the literature have been synthesized by what might be termed “conventional” coordination chemistry techniques: sources of two different metal ions and appropriate bridging and terminal ligands in a common solvent at temperatures limited by the boiling point of that solvent at atmospheric pressure. Although solvothermal methods have been used extensively to prepare *homometallic* clusters in the last 7–8 years,⁸ there is almost no work on preparing discrete M/Ln (M = a 3d metal ion) molecular clusters. Herein we report the initial use of (py)₂CO for Ni/Ln cluster chemistry under *solvothermal conditions*, which has led to a family of “star”-shaped $\{\text{Ni}_3\text{Ln}\}$ complexes with interesting structural features and magnetic properties, including SMM behavior for the $\{\text{Ni}_3\text{Dy}\}$ member.

The solvothermal reaction of Gd(NO₃)₃·6H₂O, Ni(ClO₄)₂·6H₂O, (py)₂CO, and NaO₂CMe·3H₂O (1:3:6:6) in EtOH at

(6) For example, see: Stoumpos, C. C.; Roubeau, O.; Aromi, G.; Tasiopoulos, A. J.; Nastopoulos, V.; Escuer, A.; Perlepes, S. P. *Inorg. Chem.* **2010**, *49*, 359.

(7) Efthymiou, C. G.; Georgopoulou, A. N.; Papatriantafyllopoulou, C.; Terzis, A.; Raptapoulou, C. P.; Escuer, A.; Perlepes, S. P. *Dalton Trans.* **2010**, *39*, 8603.

(8) For a minireview, see: Laye, R.; McInnes, E. J. L. *Eur. J. Inorg. Chem.* **2004**, 2811.

*To whom correspondence should be addressed. E-mail: perlepes@patreas.upatras.gr (S.P.P.), christou@chem.ufl.edu (G.C.).

(1) For reviews, see: (a) Bagai, R.; Christou, G. *Chem. Soc. Rev.* **2009**, *38*, 1011. (b) Aromi, G.; Brechin, E. K. *Struct. Bonding (Berlin)* **2006**, *122*, 1.

(2) Sessoli, R.; Powell, A. K. *Coord. Chem. Rev.* **2009**, *253*, 2328.

(3) For example, see: (a) Stamatatos, Th. C.; Teat, S. J.; Wernsdorfer, W.; Christou, G. *Angew. Chem., Int. Ed.* **2009**, *48*, 521. (b) Mereacre, V.; Ako, A. M.; Clérac, R.; Wernsdorfer, W.; Hewitt, I. J.; Anson, C. E.; Powell, A. K. *Chem.—Eur. J.* **2008**, *14*, 3577. (c) Mishra, A.; Wernsdorfer, W.; Parsons, S.; Christou, G.; Brechin, E. K. *Chem. Commun.* **2005**, 2086.

(4) For example, see: (a) Baskar, V.; Gopal, K.; Helliwell, M.; Tuna, F.; Wernsdorfer, W.; Winpenny, R. E. P. *Dalton Trans.* **2010**, *39*, 4747. (b) Abbas, G.; Lan, Y.; Mereacre, V.; Wernsdorfer, W.; Clérac, R.; Buth, G.; Sougrati, M. T.; Grandjean, F.; Long, G. J.; Anson, C. E.; Powell, A. K. *Inorg. Chem.* **2009**, *48*, 9345. (c) Chandrasekhar, V.; Pandian, B. M.; Boomishankar, R.; Steiner, A.; Vittal, J. J.; Hourii, A.; Clérac, R. *Inorg. Chem.* **2008**, *47*, 4918. (d) Costes, J.-P.; Shova, S.; Wernsdorfer, W. *Dalton Trans.* **2008**, 1843. (e) Murugesu, M.; Mishra, A.; Wernsdorfer, W.; Abboud, K. A.; Christou, G. *Polyhedron* **2006**, *25*, 613. (f) Mori, F.; Ishida, T.; Nogami, T. *Polyhedron* **2005**, *24*, 2588.

(5) Lampropoulos, C.; Stamatatos, Th. C.; Abboud, K. A.; Christou, G. *Inorg. Chem.* **2009**, *48*, 429.

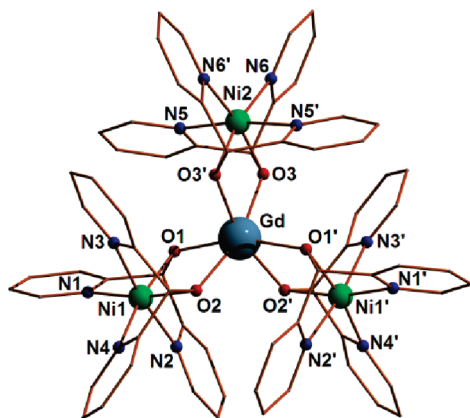


Figure 1. Partially labeled molecular structure of the cation of **1**. Primes are used for the symmetry-related ($-x, y, -z + 3/2$) atoms.

150 °C for 24 h followed by slow cooling to room temperature (see the Supporting Information, SI) gave pink crystals of $[\text{Ni}_3\text{Gd}\{(\text{py})_2\text{C}(\text{H})\text{O}\}_6](\text{ClO}_4)_3$ (**1**) in 80% yield; $(\text{py})_2\text{C}(\text{H})\text{O}^-$ is the anion of di-2-pyridylmethanol (Chart 1). The related $[\text{Ni}_3\text{Dy}\{(\text{py})_2\text{C}(\text{H})\text{O}\}_6](\text{ClO}_4)_3$ (**2**) and $[\text{Ni}_3\text{Y}\{(\text{py})_2\text{C}(\text{H})\text{O}\}_6](\text{ClO}_4)_3$ (**3**) complexes were prepared by analogous procedures. The $(\text{py})_2\text{C}(\text{H})\text{O}^-$ ion was generated by the reduction of $(\text{py})_2\text{CO}$, exploiting the enhanced reducing ability of EtOH under solvothermal conditions.⁸ Solvothermal treatment in EtOH of $(\text{py})_2\text{CO}$ without $\text{Ni}(\text{ClO}_4)_2 \cdot 6\text{H}_2\text{O}$ and with or without $\text{NaO}_2\text{CMe} \cdot 3\text{H}_2\text{O}$ both gave only unchanged $(\text{py})_2\text{CO}$ (IR and ^1H NMR evidence). In addition, **1–3** were only obtained under solvothermal conditions; under less forcing conditions, the products were Ni_2Ln complexes.⁷ Note that, although more than 10 types of in situ coordinated ligand transformations have been previously observed under hydro(solvo)thermal conditions,⁹ the present type of ketone reduction during the formation of **1–3** appears to be unprecedented. However, $(\text{py})_2\text{C}(\text{H})(\text{OH})$ has been synthesized from the reduction of $(\text{py})_2\text{CO}$ by NaBH_4 in *i*PrOH in the presence of aqueous NaOH.¹⁰

Complexes **1** (Figure 1) and **2** (Figure S1 in the SI) are isomorphous.¹¹ The four metal ions lie on a plane and are arranged in a centered triangular fashion, with the Ln at the center of a near-equilateral triangle defined by Ni1, Ni1', and Ni2 [$\text{Ni1} \cdots \text{Ni2} = 5.530(1)$ Å, $\text{Ni1} \cdots \text{Ni1}' = 5.583(1)$ Å, $\text{Ni1} - \text{Ni2} - \text{Ni1}' = 60.6(1)^\circ$, and $\text{Ni2} - \text{Ni1} - \text{Ni1}' = 59.7(1)^\circ$]. The cation is located on a 2-fold rotation axis passing through the central Gd atom and Ni2. Gd is bound by the deprotonated O atoms of the six $\eta^1:\eta^1:\eta^1:\mu-(\text{py})_2\text{C}(\text{H})\text{O}^-$ groups, which each bridge the central Ln ion to the Ni ions, forming the new $\{\text{Ni}_3\text{Ln}^{\text{III}}(\mu\text{-OR})_6\}^{3+}$ core [$\text{RO}^- = (\text{py})_2\text{C}(\text{H})\text{O}^-$]. Examination of the bond angles shows that the coordination environment of Gd approaches 3-fold symmetry.

(9) Chen, X.-M.; Tong, M.-L. *Acc. Chem. Res.* **2007**, *40*, 162.

(10) Andrade-López, N.; Alvarado-Rodríguez, J. G.; González-Montiel, S.; Páez-Hernández, M. E.; Galán-Vidal, C. A.; Jiménez-Pérez, A. *Arquív. Quím.* **2008**, *43* and references cited therein.

(11) Crystal structure data for **1**: $\text{C}_{66}\text{H}_{54}\text{Ni}_3\text{GdN}_{12}\text{O}_{18}\text{Cl}_3$, fw = 1742.94, monoclinic, space group $C2/c$ with $a = 14.746(2)$ Å, $b = 20.820(3)$ Å, $c = 23.728(4)$ Å, $\beta = 102.145(7)^\circ$, $V = 7121.7(18)$ Å³, $T = 100(2)$ K, $Z = 4$, $R1 [I > 2\sigma(I)] = 0.0377$, $wR2 (F^2, \text{all data}) = 0.0959$. Crystal structure data for **2**: $\text{C}_{66}\text{H}_{54}\text{Ni}_3\text{DyN}_{12}\text{O}_{18}\text{Cl}_3$, fw = 1748.19, monoclinic, space group $C2/c$ with $a = 14.800(2)$ Å, $b = 20.761(3)$ Å, $c = 23.681(4)$ Å, $\beta = 102.351(7)^\circ$, $V = 7107.4(16)$ Å³, $T = 100(2)$ K, $Z = 4$, $R1 [I > 2\sigma(I)] = 0.0352$, $wR2 (F^2, \text{all data}) = 0.0752$. The SQUEEZE procedure of PLATON was used to remove the disordered solvent contribution from the intensity data.

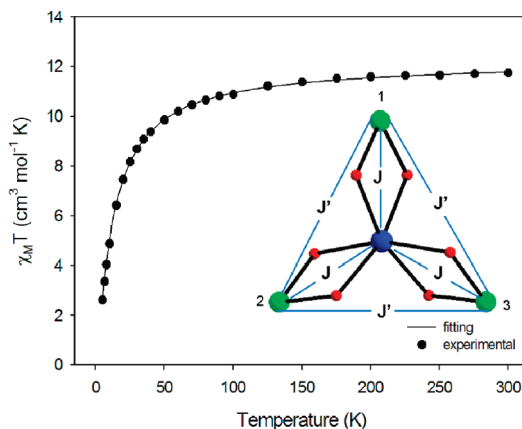


Figure 2. $\chi_M T$ vs T plot for complex **1** in a 0.1 T field. The solid line is the fit of the data in the 15–300 K range to the theoretical expression for the $2 - J$ model shown; see the text for the fit parameters.

The GdO1O2Ni1 rhombus is near-planar and forms dihedral angles of $77.3(1)$ and $78.2(1)^\circ$ with the GdO3O3'Ni2 and GdO1'O2'Ni1' planes, respectively. Consequently, the cation has a propeller shape with virtual D_3 symmetry and is chiral. Because the space group is centrosymmetric, both enantiomeric forms are present in the crystal. The cations of **1** form chains through intermolecular π – π -stacking interactions, while $\text{C-H} \cdots \pi$ supramolecular interactions link the chains, forming a 2D network (Figure S2 in the SI). The $\{\text{M}_4\}$ centered-triangle topology with exclusively monoatomic bridges, commonly called the “metal star” topology, is known for $\{\text{M}_4\}^{12a,b}$ and $\{\text{M}_3\text{M}'\}^{12c}$ clusters, where M and M' are transition-metal ions. Complexes **1** and **2** are thus the first such clusters with a central Ln^{III} and three outer transition-metal ions.

Solid-state direct-current (dc) magnetic susceptibility (χ_M) data on **1–3** were collected in a 0.1 T field in the 5.0–300 K range and are plotted as $\chi_M T$ vs T for **1** in Figure 2. $\chi_M T$ for **1** is $11.75 \text{ cm}^3 \text{ K mol}^{-1}$ at 300 K, remains almost constant down to ~ 100 K, and then rapidly decreases to $2.64 \text{ cm}^3 \text{ K mol}^{-1}$ at 5.0 K. The 300 K value is slightly lower than the $12.57 \text{ cm}^3 \text{ K mol}^{-1}$ expected for one Gd^{III} ($S = 7/2$ and $L = 0$) and three Ni^{II} ($S = 1$) noninteracting ions, assuming an average g value¹³ of 2.15. To determine the individual pairwise exchange parameters J and J' between the Gd–Ni and Ni–Ni pairs, respectively, the $\chi_M T$ vs T data were fit to the appropriate theoretical expression. Given the high symmetry of the cluster cation, the nearly equal Ni–(OR)₂–Gd angles, and the fact that the $\text{Ni} \cdots \text{Ni}$ interactions are not negligible, as judged from the study of **3** (vide infra), we employed a $2 - J$ model (inset to Figure 2). The corresponding isotropic spin Hamiltonian is given by eq 1, where \hat{S}_i is the spin operator for metal M_i ($i = 1–3$ for Ni and 4 for Gd).

$$\mathcal{H} = -2J(\hat{S}_1 \cdot \hat{S}_4 + \hat{S}_2 \cdot \hat{S}_4 + \hat{S}_3 \cdot \hat{S}_4) - 2J'(\hat{S}_1 \cdot \hat{S}_2 + \hat{S}_2 \cdot \hat{S}_3 + \hat{S}_1 \cdot \hat{S}_3) \quad (1)$$

(12) (a) Tidmarsh, I. S.; Batchelor, L. J.; Scales, E.; Laye, R. H.; Sorace, L.; Caneschi, A.; Schnack, J.; McInnes, E. J. L. *Dalton Trans.* **2009**, 9402. (b) Accorsi, S.; Barra, A.-L.; Caneschi, A.; Chastanet, G.; Cornia, A.; Fabretti, A. C.; Gatteschi, D.; Mortal, C.; Olivieri, E.; Parenti, F.; Rosa, P.; Sessoli, R.; Sorace, L.; Wernsdorfer, W.; Zolbi, L. *J. Am. Chem. Soc.* **2006**, *128*, 4742. (c) Saalfrank, R. W.; Bernt, I.; Chowdhry, M. M.; Hampel, F.; Vaughan, G. B. M. *Chem.—Eur. J.* **2001**, *7*, 2765.

(13) Yukawa, Y.; Aromi, G.; Igarashi, S.; Ribas, J.; Zvyagin, S. A.; Krzystek, J. *Angew. Chem., Int. Ed.* **2005**, *44*, 1997.

Communication

The eigenvalues of this spin Hamiltonian can be determined analytically with the Kambe vector coupling method and the substitutions $\hat{S}_A = \hat{S}_1 + \hat{S}_2 + \hat{S}_3$ and $\hat{S}_T = \hat{S}_A + \hat{S}_4$, where S_T is the total spin of the cation. The spin Hamiltonian is transformed into the equivalent form given by eq 2, and its eigenvalues are given by eq 3, where $E(S_T, S_A)$ is the energy of state S_T arising from S_A and constant terms contributing to all states have been omitted.

$$\mathcal{H} = -J(\hat{S}_T^2 - \hat{S}_A^2 - \hat{S}_4^2) - J'(\hat{S}_A^2 - \hat{S}_1^2 - \hat{S}_2^2 - \hat{S}_3^2) \quad (2)$$

$$E(S_T, S_A) = -J[S_T(S_T + 1) - S_A(S_A + 1)] - J'[S_A(S_A + 1)] \quad (3)$$

For complex **1**, the overall multiplicity of the spin system is 216, made up of 27 individual spin states ranging from $S_T = 1/2$ to $13/2$. These were used to derive the appropriate van Vleck equation, which was used to fit the $\chi_M T$ vs T data in the 15–300 K range, giving fit parameters of $J = -1.09(7) \text{ cm}^{-1}$, $J' = -0.99(7) \text{ cm}^{-1}$, and $g = 2.11(6)$ (solid line in Figure 2). A temperature-independent paramagnetism (TIP) term was included and held constant at $400 \times 10^{-6} \text{ cm}^3 \text{ mol}^{-1}$. The exchange interactions thus both are weakly antiferromagnetic and indicate the complex to have the $|S_T, S_A\rangle = |1/2, 3\rangle$ ground state, with the $|3/2, 3\rangle$ first excited state at 3.27 cm^{-1} above the ground state. The $S_T = 1/2$ ground state was confirmed by the alternating-current (ac) magnetic susceptibility data (Figure S4 in the SI). Most of the reported $\text{Ni}^{\text{II}} \cdots \text{Gd}^{\text{III}}$ interactions in the literature are weakly ferromagnetic,^{4c,7} but recently antiferromagnetic ones have also been reported.¹⁴

For isostructural **3**, the Y^{III} ion is diamagnetic, allowing independent assessment of the exchange interactions between the peripheral Ni^{II} ions. Following the above procedure but with $J = 0$ in eqs 1–3 allows the corresponding van Vleck equation to be derived. The subsequent fit of the data (solid line in Figure S3 in the SI) gave $J' = -0.41(1) \text{ cm}^{-1}$ and $g = 2.16(1)$. A nonnegligible J' for the GdNi_3 complex **1** is thus independently supported.

$\chi_M T$ for **2** at 300 K is $20.29 \text{ cm}^3 \text{ K mol}^{-1}$, slightly larger than the $\sim 17.8 \text{ cm}^3 \text{ K mol}^{-1}$ value expected for one Dy^{III} ($^6\text{H}_{15/2}$ free ion, $S = 5/2$, $L = 5$, and $g_J = 4/3$) and three Ni^{II} ($S = 1$) noninteracting ions, probably from the spin–orbit effects of the Dy^{III} ion in a distorted octahedral crystal field. It decreases gradually with decreasing temperature to $8.02 \text{ cm}^3 \text{ K mol}^{-1}$ at 5.0 K (Figure S5 in the SI) because of depopulation of the Stark sublevels of the $\text{Dy}^{\text{III}} ^6\text{H}_{15/2}$ state and $\text{Ni}^{\text{II}} \cdots \text{Dy}^{\text{III}}$ antiferromagnetic interactions. $\chi_M T$ at 5.0 K and the ac in-phase $\chi_M' T$ down to 1.8 K (Figure S6 in the SI) indicate significant remaining paramagnetism at the

(14) Georgopoulou, A. N.; Adam, R.; Raptopoulou, C. P.; Psycharis, V.; Ballesteros, R.; Abarca, B.; Boudalis, A. K. *Dalton Trans.* **2010**, 39, 5020.

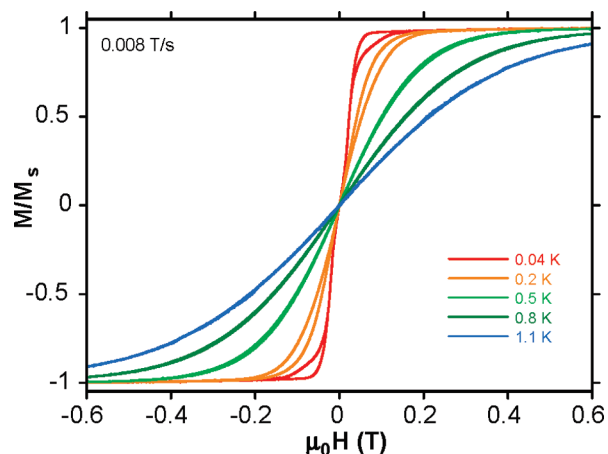


Figure 3. Magnetization (M) vs applied dc field H hysteresis loops for a single crystal of **2** at 0.008 T/s and the indicated temperatures. The magnetization is normalized to its saturation value M_s .

lowest temperatures. The ac out-of-phase susceptibility (χ_M'' ; Figure S7 in the SI) displays frequency-dependent signals (but no peaks) below ~ 3 K, possibly indicative of SMM behavior. To probe the latter further, data were collected on a single crystal of **2** down to 0.04 K using a micro-SQUID apparatus.¹⁵ Weak magnetization hysteresis was observed (Figures 3 and S8 and S9 in the SI) at ≤ 0.2 K, exhibiting increasing coercivity with decreasing temperature and with increasing sweep rate, as expected for the superparamagnet-like behavior of an SMM. The dominating feature of the sweeps is the large relaxation at zero field assignable to fast quantum tunneling of the magnetization.^{4d,e} The first step in sweeping the field from one saturating value to another does not occur at zero field, assignable to weak intermolecular antiferromagnetic exchange interactions, as suggested by the crystal structure.^{4c} Complex **2** is the first Ni/Ln SMM^{4c,f} for which hysteresis loops have been recorded.

In conclusion, novel “star”-shaped $\{\text{Ni}_3\text{Ln}\}$ clusters have resulted from the in situ reduction of di-2-pyridyl ketone under solvothermal conditions. This suggests that a synthetic method using other polydentate ketones as proligands under solvothermal conditions is a promising route toward transition-metal/lanthanide clusters with new topologies and interesting magnetic properties.

Acknowledgment. This work was supported by NSF Grant CHE-0910472 (to G.C.) and the Cyprus Research Promotion Foundation (Grant DIETHNIS/STOXOS/0308/14).

Supporting Information Available: Crystallographic data (CIF format), a general synthetic procedure and microanalyses for **1–3**, and structural (Figures S1 and S2) and magnetic (Figures S3–S9) figures. This material is available free of charge via the Internet at <http://pubs.acs.org>.

(15) Wernsdorfer, W. *Adv. Chem. Phys.* **2001**, 118, 99.